

# Can Vision-Language Models Handle Long-Context Code? An Empirical Study on Visual Compression

JIANPING ZHONG, Zhejiang University, Ningbo, China

GUOCHANG LI, Zhejiang University, Hangzhou, China

CHEN ZHI\*, Zhejiang University, Ningbo, China

JUNXIAO HAN, Hangzhou City University, Hangzhou, China

ZHEN QIN, Zhejiang University, Ningbo, China

XINKUI ZHAO, Zhejiang University, Ningbo, China

NAN WANG, Shenzhou Aerospace Software Technology Company Limited, Beijing, China

SHUIGUANG DENG, Zhejiang University, Hangzhou China

JIANWEI YIN, Zhejiang University, Hangzhou, China

Large Language Models (LLMs) struggle with long-context code due to window limitations. Existing textual code compression methods mitigate this via selective filtering but often disrupt dependency closure, causing semantic fragmentation. To address this, we introduce LongCodeOCR, a visual compression framework that renders code into compressed two-dimensional image sequences for Vision-Language Models (VLMs). By preserving a global view, this approach avoids the dependency breakage inherent in filtering. We systematically evaluate LongCodeOCR against the state-of-the-art LongCodeZip across four benchmarks spanning code summarization, code question answering, and code completion.

Our results demonstrate that visual code compression serves as a viable alternative for tasks requiring global understanding. At comparable compression ratios ( $\sim 1.7\times$ ), LongCodeOCR improves CompScore on Long Module Summarization by 36.85 points over LongCodeZip. At a 1M-token context length with Glyph (a specialized 9B VLM), LongCodeOCR maintains higher accuracy than LongCodeZip while operating at about  $4\times$  higher compression. Moreover, compared with LongCodeZip, LongCodeOCR drastically reduces compression-stage overhead (reducing latency from  $\sim 4.3$  hours to  $\sim 1$  minute at 1M tokens). Finally, our results characterize a fundamental coverage-fidelity trade-off: visual code compression retains broader context coverage to support global dependencies, yet faces fidelity bottlenecks on exactness-critical tasks; by contrast, textual code compression preserves symbol-level precision while sacrificing structural coverage.

Additional Key Words and Phrases: large language models, visual code compression, long-context code understanding

---

\*Chen Zhi is the corresponding author.

---

Authors' Contact Information: Jianping Zhong, Zhejiang University, Ningbo, China, [jpz@zju.edu.cn](mailto:jpz@zju.edu.cn); Guochang Li, Zhejiang University, Hangzhou, China, [gcl@zju.edu.cn](mailto:gcl@zju.edu.cn); Chen Zhi, Zhejiang University, Ningbo, China, [zjuzhichen@zju.edu.cn](mailto:zjuzhichen@zju.edu.cn); Junxiao Han, Hangzhou City University, Hangzhou, China, [hanjx@hzcu.edu.cn](mailto:hanjx@hzcu.edu.cn); Zhen Qin, Zhejiang University, Ningbo, China, [zhenqin@zju.edu.cn](mailto:zhenqin@zju.edu.cn); Xinkui Zhao, Zhejiang University, Ningbo, China, [zhaoxinkui@zju.edu.cn](mailto:zhaoxinkui@zju.edu.cn); Nan Wang, Shenzhou Aerospace Software Technology Company Limited, Beijing, China, [wangnan02026@163.com](mailto:wangnan02026@163.com); Shuiguang Deng, Zhejiang University, Hangzhou China, [dengsg@zju.edu.cn](mailto:dengsg@zju.edu.cn); Jianwei Yin, Zhejiang University, Hangzhou, China, [zjuyjw@cs.zju.edu.cn](mailto:zjuyjw@cs.zju.edu.cn).

---

Permission to make digital or hard copies of all or part of this work for personal or classroom use is granted without fee provided that copies are not made or distributed for profit or commercial advantage and that copies bear this notice and the full citation on the first page. Copyrights for components of this work owned by others than the author(s) must be honored. Abstracting with credit is permitted. To copy otherwise, or republish, to post on servers or to redistribute to lists, requires prior specific permission and/or a fee. Request permissions from [permissions@acm.org](mailto:permissions@acm.org).

© 2026 Copyright held by the owner/author(s). Publication rights licensed to ACM.

ACM XXXX-XXXX/2026/2-ART

<https://doi.org/10.1145/nnnnnnnn.nnnnnnnn>

**ACM Reference Format:**

Jianping Zhong, Guochang Li, Chen Zhi, Junxiao Han, Zhen Qin, Xinkui Zhao, Nan Wang, Shuiguang Deng, and Jianwei Yin. 2026. Can Vision-Language Models Handle Long-Context Code? An Empirical Study on Visual Compression. 1, 1 (February 2026), 21 pages. <https://doi.org/10.1145/nnnnnnnn.nnnnnnn>

## 1 Introduction

In recent years, Large Language Models (LLMs) for code have made substantial progress on tasks such as code completion[19, 29], program synthesis[47], program repair[7, 23], unit test generation[8] and LLM-based application analysis[42], significantly advancing the development of intelligent developer assistant tools. As application scenarios evolve from single-file scopes to repository-scale, models increasingly need to resolve cross-file evidence, including API definitions, complex call relationships, and configuration scripts. Such critical signals are often scattered across multiple files and locations, causing the required input context to frequently grow to tens of thousands of tokens or more. However, feeding such long contexts directly into LLMs creates a fundamental tension between information integrity and computational feasibility. Specifically: (1) under the standard Transformer architecture, the computational complexity of the self-attention mechanism[37] grows quadratically with sequence length, leading to prohibitive memory footprints and inference latency; (2) in long and noisy inputs, evidence localization becomes unreliable[25], a phenomenon known as “lost-in-the-middle”[28]; and (3) contexts may still exceed hard window limits, where forced truncation disrupts the dependency closure of the code, thereby leading to reasoning failure.[5]

However, there has been limited progress in addressing long context limitations for code. General text compression methods like LLMLingua[20] and Selective Context[26] fail to account for code-specific characteristics and often break syntactic validity. Retrieval-augmented generation (RAG)[11] may overlook implicit dependencies within the context. Existing code compression methods, such as DietCode [48], SlimCode [40], and LongCodeZip [36], compress long contexts by selectively pruning or filtering less useful code snippets. By relying on binary keep-or-discard decisions, these methods inevitably fragment the context. More fundamentally, these existing methods can be unified under a single paradigm—textual code compression. This classification arises because they primarily operate on one-dimensional token sequences via selective filtering.

Meanwhile, vision-text compression (VTC), also known as contextual optical compression, has emerged as a promising cross-modal paradigm for mitigating context limitations recently. By rendering long documents into compressed two-dimensional image sequences, VTC replaces token-level pruning with visual representations under a fixed visual token budget, as explored in DeepSeek-OCR [41], AgentOCR[17] and Glyph [10]. This approach avoids the dependency breakage inherent in selective filtering by preserving a global view of the code context. However, the applicability of VTC to code understanding remains insufficiently characterized. Unlike natural language, code understanding requires strict symbol-level fidelity, and even a single missing operator or an ambiguously rendered character can break syntactic validity and compromise downstream reasoning. It therefore remains unclear whether visual code compression can balance the trade-off between global context coverage and the high-fidelity precision required for code understanding.

To bridge the gap, we present LongCodeOCR, a visual compression framework that renders code into compressed two-dimensional image sequences for Vision-Language Models (VLMs), and conduct a systematic empirical study on realistic SE datasets. We evaluate on a diverse suite of long-context code benchmarks spanning task types and context scales: Long Module Summarization[5] for assessing global semantic abstraction, LongCodeQA[35] for measuring cross-file reasoning, and both Long Code Completion[19] and RepoBench-P[3] for evaluating strict syntactic precision.

By rendering these multi-scale contexts into images for VLM inference, we conduct an in-depth empirical examination of the visual paradigm across diverse software engineering tasks.

Through data analysis, we have summarized several insights. First, visual code compression is more suitable for tasks that require broad semantic coverage and constraint grounding, whereas textual code compression tends to work better when the required evidence is sparse and locally salient. Second, visual code compression exhibits more stable performance than textual code compression as context length increases, and its relative advantage becomes more pronounced for ultra-long inputs. Third, visual code compression is governed by a fundamental coverage–fidelity trade-off: it benefits global-dependency scenarios by preserving context coverage, but can face a fidelity bottleneck on exactness-critical tasks. In contrast, textual code compression primarily trades coverage for compression, while visual compression primarily trades symbol-level fidelity.

Our contributions can be summarized as follows:

- We conduct a systematic empirical study of visual code compression for long-context code understanding.
- We develop LongCodeOCR, a global-preserving visual code compression framework, and evaluate it on four representative long-context benchmarks spanning code summarization, code question answering, and code completion.
- We analyze how visual code compression and textual code compression differ in preserving dependency-critical information, and discuss implications for designing reliable long-context code compression methods.

The rest of the paper is organized as follows: Section 2 introduces the limitations of LongCodeZip. Section 3 presents an overview of the LongCodeOCR framework. Section 4 describes our empirical study design. Section 5 records the experimental results and analyzes our findings. Section 6 discusses the implications of our findings and potential threats to validity. Section 7 reviews related work concerning long-context code benchmarks, efficient long-context architectures and existing context compression paradigms. Section 8 concludes the paper.

## 2 Limitations of Selective Filtering in Long-Context Code Compression

LongCodeZip[36] serves as a strong and representative baseline for long-context code compression. It adopts a coarse-to-fine pipeline: it first scores and ranks function-level chunks with Approximate Mutual Information (AMI), and then performs budget-constrained intra-function selection via 0–1 knapsack optimization. Overall, this procedure instantiates a token-budgeted *hard selection* strategy—i.e., *selective filtering-based compression*—where a fixed budget is met through largely irreversible keep-or-discard decisions over candidate units (e.g., functions, chunks, and blocks) guided by model-derived relevance estimates.

Although such filtering can improve performance on average, rigidly separating code into **relevant** and **irrelevant** buckets incurs intrinsic risks. In particular, it may fragment the available evidence and weaken the structural integrity required for reliable reasoning: semantic dependencies often span multiple units, yet each unit can appear weakly informative when evaluated in isolation. We next analyze these limitations along two dimensions: **Semantic Fragmentation** (§2.1) and **Preprocessing Overhead** (§2.2).

### 2.1 How Selective Filtering Causes Semantic Fragmentation

In LongCodeZip, AMI offers an actionable ranking signal by approximating how much a candidate chunk reduces the conditional perplexity of a task-relevant target sequence. However, this choice exposes a fundamental mismatch: perplexity-based “contribution” does not necessarily capture whether a chunk is a semantic prerequisite for solving the task.

Table 1. Compression overhead of selective filtering-based compression. We report compression-stage latency and LLM token usage across input lengths. Lower values indicate lower overhead, the best (lowest) values are bolded.

| Method                                     | Tokens are reported in millions (M). |             |             |             |             |              |              |
|--|--------------------------------------|-------------|-------------|-------------|-------------|--------------|--------------|
|  | 8k                                   | 16k         | 32k         | 64k         | 128k        | 512k         | 1M           |
| <b>Compression-stage Latency (seconds)</b> |                                      |             |             |             |             |              |              |
| LongCodeZip (coarse)                       | 2.87                                 | 12.41       | 13.00       | 24.70       | 40.86       | 163.50       | 254.85       |
| LongCodeZip (fine)                         | 24.05                                | 67.56       | 157.90      | 377.91      | 2774.14     | 7246.67      | 15154.77     |
| LongCodeZip (total)                        | 26.97                                | 80.05       | 171.06      | 402.89      | 2815.52     | 7413.15      | 15415.53     |
| <b>Visual code compression (total)</b>     | <b>0.84</b>                          | <b>1.52</b> | <b>2.79</b> | <b>5.30</b> | <b>9.35</b> | <b>37.20</b> | <b>70.36</b> |
| <b>Compression-stage LLM Tokens (M)</b>    |                                      |             |             |             |             |              |              |
| LongCodeZip (tokens)                       | 0.17                                 | 0.44        | 2.32        | 7.71        | 79.91       | 172.77       | 221.76       |
| <b>Visual code compression (tokens)</b>    | <b>0</b>                             | <b>0</b>    | <b>0</b>    | <b>0</b>    | <b>0</b>    | <b>0</b>     | <b>0</b>     |

In long-context code understanding, many prerequisites take the form of *dispersed and low-salience constraints*—e.g., configuration guards, interface contracts, error-handling conditions, cross-cutting constants, and implicit invariants. These constraints can be decisive for solvability and correctness, yet their utility is often *non-local*: their effect becomes apparent only when multiple dependent units are available simultaneously. When candidates are ranked at chunk granularity, such prerequisites may yield small or unstable AMI estimates and are thus ranked behind locally predictive fragments; consequently, they are easily filtered out.

Figure 1 concretely illustrates this failure mode of selective filtering. In the original context (left), the highlighted class definition of SingleCellSelection provides a prerequisite for correct completion, namely the constructor signature SingleCellSelection(ILayerCell cell). Although this snippet may appear weakly informative when scored in isolation, it is structurally necessary to ground the correct instantiation (bottom, ground truth). After selective filtering (right), the definition is removed, leaving a masked region that indicates missing evidence for a valid initialization. With the constructor information no longer available in the remaining context, the model backs off to an alternative class (SelectCellCommand; bottom, model output), resulting in a reasoning failure and an incorrect completion.

More broadly, source code imposes strong *dependency-closure* requirements: syntax completeness, scope and name binding, type and symbol resolution, and data-flow dependencies constrain which evidence must co-occur to enable correct completion. *Selective filtering-based compression* deletes units irreversibly and can therefore break dependency closure—for example, retaining a call site while dropping the callee definition. **Once a prerequisite is removed, downstream models cannot reconstruct the missing evidence, creating an unrecoverable recall gap that bounds achievable reliability.**

## 2.2 Time and Token Cost of the Compression Stage

In long-context code tasks, selective filtering-based compression typically relies on fine-grained scoring and comparison over a large pool of candidate units. To obtain a ranking signal suitable for *selective filtering*, the compressor must run many model forward passes (e.g., estimating conditional perplexity differences) across candidates. **As a result, compression itself becomes a computational bottleneck, whose cost grows rapidly with context length.**

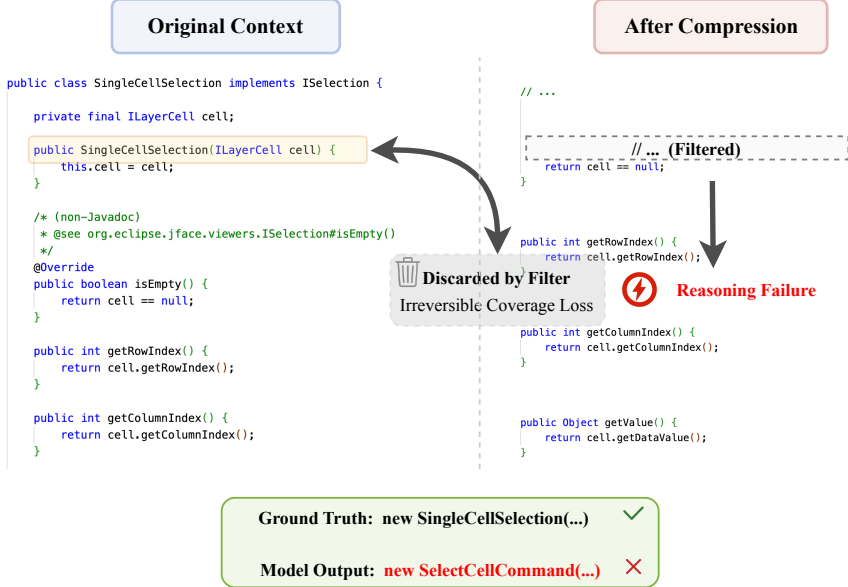


Fig. 1. A motivating example from RepoBench-P illustrating how selective filtering can break dependency closure. The `SingleCellSelection` definition (left, highlighted) is required for correct code completion but is removed after filtering (right, indicated by the masked region), causing irreversible coverage loss and an incorrect completion.

This compression-phase inference overhead directly translates into preprocessing latency, which is difficult to reconcile with interactive workflows that require near real-time responses. Table 1 quantifies the preprocessing burden of selective filtering-based compression. For LongCodeZip, the coarse ranking stage grows moderately with length (13.00 seconds at 32k to 40.86 seconds at 128k), whereas the fine-grained selection stage dominates the compression-stage latency. At 128k, fine-grained selection takes 2774.14 seconds out of a total of 2815.52 seconds (**98.5%**), already pushing preprocessing to  $\sim$ 47 min. At 1M, the total compression time further reaches 15415.53 seconds ( $\sim$ 4.3 h), with 15154.77 seconds spent in the fine-grained stage. Meanwhile, compression-stage LLM token usage also scales sharply, from 2.32M tokens at 32k to 79.91M at 128k and 221.76M at 1M. **These results indicate that compute pressure is not removed but shifted to the compression phase, making it difficult to achieve both high fidelity and interactive latency.**

By contrast, our approach completes compression in 70.36 seconds at 1M without any compression-stage LLM calls (0 tokens). For LongCodeZip, a latency-oriented alternative is to adopt coarse-grained filtering. However, such strategies provide limited support for preserving cross-unit dependencies and dependency closure, and thus frequently sacrifice fidelity for speed, resulting in a characteristic *efficiency–fidelity* trade-off under ultra-long contexts.

Taken together, selective filtering-based compression can be brittle under evidence fragmentation and can incur substantial preprocessing overhead at ultra-long lengths, motivating alternative representations that preserve global structure.

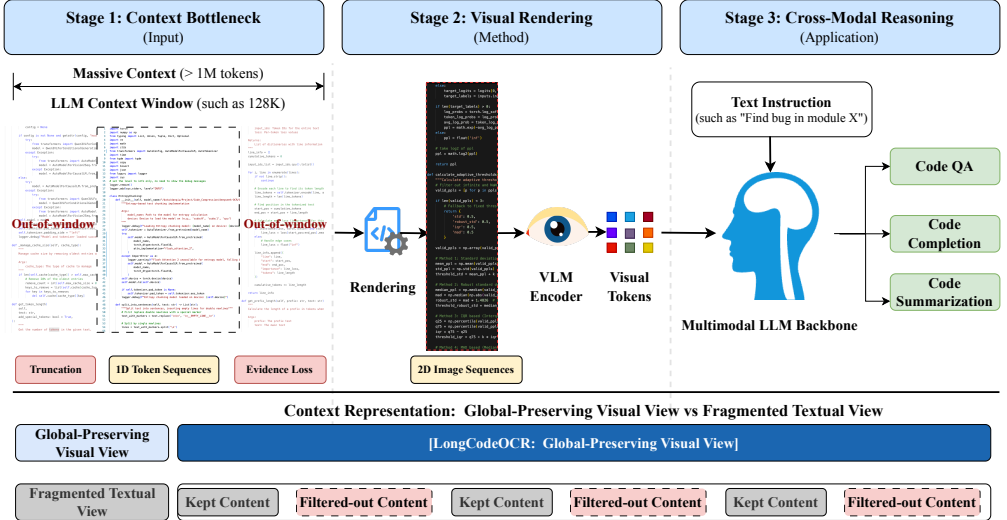


Fig. 2. Framework overview of LongCodeOCR and two paradigms for long-context code compression. Stages 1–3 depict how massive code contexts are rendered into a 2D image sequences and encoded into visual tokens for instruction-conditioned, cross-modal reasoning. The bottom panel highlights the contrast between the global-preserving visual view and the fragmented textual view.

### 3 Framework Overview

We study context compression for long-context code understanding through two paradigms: **textual code compression, which yields a fragmented textual view, and visual code compression, which maintains a global-preserving visual view**. Figure 2 overviews the LongCodeOCR pipeline (Stages 1–3) and highlights the structural contrast between the fragmented textual snippets resulting from selective filtering and our unified, global-preserving visual view under the same input budget.

*Stage 1: Context Bottleneck (Input).* As shown in the left panel of Figure 2, real-world repositories can induce massive contexts that exceed the context window of standard text-only LLMs. Under a fixed window (such as 128K tokens), code is processed as a 1D token sequences, and length control typically relies on truncation or selective filtering. As a result, out-of-window content is omitted, which can cause evidence loss when task-critical prerequisites fall outside the retained context.

*Stage 2: Visual Rendering (Method).* LongCodeOCR implements global-preserving visual compression by rendering code into a compact 2D image sequences. A vision-language encoder converts the rendered view into a sequence of visual tokens, providing a high-density representation within the same input constraint. Unlike selective filtering on a 1D token sequences, this stage densifies context without requiring fine-grained keep-or-discard decisions over code units.

*Stage 3: Cross-Modal Reasoning (Application).* In the right panel of Figure 2, a multimodal LLM backbone performs instruction-conditioned fusion between the text instruction and the encoded visual tokens. The model then generates task-specific outputs for downstream SE tasks, including code QA, code completion, and code summarization.

*Context representation: global-preserving visual view vs. fragmented textual view.* The bottom panel of Figure 2 summarizes the contrast between the two paradigms:

- **Textual Code Compression.** This paradigm meets the input constraint via keep-or-discard decisions over candidate units, producing kept content interleaved with filtered-out content. Because semantic dependencies can span multiple units, selective filtering may remove task-critical prerequisites, weakening dependency closure and reducing reliability.
- **Visual Code Compression.** In contrast, LongCodeOCR renders the context into a global-preserving view and encodes it as visual tokens, yielding a more contiguous representation of global structure under the same constraint. This approach avoids the dependency breakage inherent in selective filtering by preserving a global view of the context.

In this study, we instantiate the visual code compression paradigm through a proposed framework, LongCodeOCR. We use LongCodeOCR as the primary vehicle to empirically evaluate the efficacy of the visual paradigm against textual code compression methods.

## 4 Study Design

### 4.1 Datasets

We study three representative long-context code understanding tasks: code summarization for assessing global semantic abstraction, code question answering for measuring cross-file reasoning, and code completion for evaluating strict syntactic precision. Collectively, these tasks evaluate whether a compressed context preserves task-critical evidence for reliable performance in developer-facing scenarios.

For the code summarization task, we adopt the Long Module Summarization dataset[5], which targets project-level documentation generation given a project code context and a one-sentence *intent*. To target challenging long-context settings, we retain only 139 instances whose contexts exceed 2,000 tokens.

For the code question answering task, we adopt LongCodeQA[35], a four-option multiple-choice benchmark for evaluating long-context code understanding and reasoning. Each instance includes an instruction, a filename-sorted set of repository files, and a question derived from resolved issues in public GitHub Python repositories via an automated pipeline; questions that remain answerable without repository context are removed. The benchmark contains 443 instances from 98 repositories and is balanced across context-length ranges.

For the code completion task, we evaluate it across two distinct scopes: **file-level**, which focuses on internal consistency, and **repository-level**, which demands cross-file reasoning.

- **Long Code Completion (File-level context).** Introduced in LongCoder [19], Long Code Completion(LCC) targets completion within a single file. It evaluates the model’s capacity to maintain local semantic consistency while capturing *long-range constraints* appearing earlier in the same file. To emphasize long-context difficulty, we restrict the test set to 500 Python instances whose input contexts exceed 5,000 tokens.
- **RepoBench-P (Repository-level context).** Adapted from LongBench [3], this benchmark targets completion requiring *cross-file evidence*. Unlike LCC, it constructs inputs by retrieving relevant fragments from external files (e.g., via import statements). We specifically employ the **XF-F (Cross-File-First)** setting, where within-file context alone is insufficient, thereby directly assessing the model’s ability to integrate and leverage distributed dependencies.

### 4.2 Model and Baseline Selection

4.2.1 *Baseline Selection.* We evaluate LongCodeOCR against a variety of competitive baselines:

- **No Compression:** We provide the full code context without applying any compression.

- **Random Baseline:** Random Line removes complete lines of code uniformly at random.
- **Retrieval-based Methods:** We instantiate two RAG variants: RAG (Sliding Window) segments the context into fixed-size overlapping chunks, whereas RAG (Function Chunking) splits code at function boundaries. Both variants represent chunks with UniCoder-base and select the top- $k$  chunks by instruction–chunk similarity for concatenation.[18, 46]
- **Text Compression Methods:** We apply representative prompt-compression methods to the code context, including LLMLingua [20], LongLLMLingua [21], and LLMLingua-2[32].
- **Code Compression Methods:** We include LongCodeZip [36] as a strong code-aware compression baseline. It implements a coarse-to-fine pruning strategy that filters context by ranking function-level chunks via approximate mutual information and performing fine-grained block selection to retain instruction-relevant spans.

4.2.2 *Model Selection.* We evaluate open-source models of similar parameter scales to isolate the effect of context representation on long-context code tasks under a consistent evaluation protocol. In particular, we compare the same code context represented as plain text versus as rendered images. Specifically, we use Qwen3-8B[44] as the text-only LLM baseline, and include two vision–language models (VLMs) as multimodal counterparts: Qwen3-VL-8B[1] and Glyph[10] (9B). Qwen3-VL-8B serves as a general-purpose VLM baseline for direct visual code understanding with off-the-shelf multimodal capabilities. In contrast, Glyph is a long-context-oriented VLM designed for visual compression: it employs an LLM-guided search to tune rendering configurations and is trained with a dedicated vision–text alignment curriculum. Together, these components enable Glyph to encode substantially more textual evidence into a compact visual token budget than a general-purpose VLM. Although Glyph is slightly larger than the 8B baselines, they remain within a comparable parameter regime, enabling a fair contrast between general-purpose and specialized visual compression models under similar capacity constraints. To ensure rigorous comparison, we employ identical prompt templates and consistent evaluation protocols across all tasks.

### 4.3 Evaluation Metrics

4.3.1 *Compression Ratio.* We evaluate compression ratios across two input modalities: (i) visual code compression, where contexts are rendered and encoded as visual tokens (represented by LongCodeOCR), and (ii) textual code compression, where contexts are reduced via pruning or filtering (represented by LongCodeZip and other baselines).

**Visual code compression.** For the visual code compression method, let  $C_{\text{context}}$  denote the *token sequence* of the original code context, counted using the tokenizer of the evaluated VLM. After rendering, the code context is represented as a sequence of  $n$  images  $\mathcal{V} = \{v_i\}_{i=1}^n$ .

To quantify the information cost, we adopt the estimation formula from VTCBench [49]. We abstract away model-specific resizing and assume each page  $v_i$  has resolution  $(H_i, W_i)$ . The *estimated* number of visual tokens  $\tau(v_i)$  consumed by the VLM is calculated as:

$$\tau(v_i) = \begin{cases} \frac{H_i \cdot W_i}{16 \cdot 16 \cdot 4}, & \text{Qwen3-VL-8B [1]} \\ \frac{H_i \cdot W_i}{14 \cdot 14 \cdot 4}, & \text{Glyph [10]} \end{cases} \quad (1)$$

where the denominator factors account for the patch size ( $16^2$  or  $14^2$ ) and the  $2 \times 2$  pooling mechanism (factor 4) inherent to the VLM architectures.

The total visual token count is  $|C_{\text{visual}}| = \sum_{i=1}^n \tau(v_i)$ . The compression ratio is computed as:

$$\text{Ratio}_{\text{visual}} = \frac{|C_{\text{context}}|}{|C_{\text{visual}}|} \quad (2)$$

Table 2. Rendered context fields and benchmark-level average compression ratios.

| Task                    | Dataset                   | Rendered context field | Avg. ratio |
|-------------------------|---------------------------|------------------------|------------|
| Code Summarization      | Long Module Summarization | context                | 1.7        |
| Code Question Answering | LongCodeQA                | repo_text              | 1.6        |
| Code Completion         | Long Code Completion      | background_context     | 2.0        |
|                         | RepoBench-P               | context                | 2.0        |

where  $|C_{\text{context}}|$  and  $|C_{\text{visual}}|$  denote the total token counts of the original code context and the rendered visual context, respectively.

**Textual code compression.** For the textual code compression methods, the ratio is defined as:

$$\text{Ratio}_{\text{textual}} = \frac{|C_{\text{context}}|}{|C_{\text{compressed}}|} \quad (3)$$

where  $|C_{\text{compressed}}|$  denotes the token count of the compressed context.

**4.3.2 Downstream Task Performance.** We evaluate downstream performance using task-specific metrics.

For the code summarization task, we follow [5] and use GPT-4o-mini [31] as a third-party referee model to perform pairwise comparison between the generated summary  $s_o$  and the reference summary  $\hat{s}$ , conditioning on the code. To mitigate order bias, we query the referee twice with reversed order. We then compute *CompScore* as:

$$\text{CompScore} = \frac{1}{2} \left[ P(s_o \succ \hat{s}) + (1 - P(\hat{s} \succ s_o)) \right], \quad (4)$$

where  $P(s_o \succ \hat{s})$  is the probability that the referee prefers  $s_o$  over  $\hat{s}$ , and  $P(\hat{s} \succ s_o)$  is the probability under the reversed order. CompScore ranges from 0 to 100, with 50 indicating equal preference.

For the code completion task, we follow benchmark-specific evaluation protocols: for LCC, we follow LongCoder [19] to evaluate model performance using Exact Match (EM) and Edit Similarity (ES). For RepoBench-P, we follow LongBench [3] to evaluate model performance using ES.

For the code question answering task, we follow LongCodeBench [35] to report answer accuracy.

#### 4.4 Implementation Details

To avoid introducing answer-related information during visualization and to ensure a fair comparison, we render only the long code context that serves as model input into images for VLM-based methods. Non-code inputs, such as task instructions, intents, and candidate options, are kept in text form. LLM baselines and VLM-based methods are provided with the same information; they differ only in how the long context is represented (text vs. images).

For the LCC task, the function to be completed appears at the end of the sample context. Rendering the entire context may expose the target code and thus cause information leakage. Following the processing protocol of LongCodeZip [36], we split the target function from the original sample and render only the preceding code snippet as the visualized context (i.e., `background_context`). The model is tasked with completing the separated target function implementation given this context.

Table 2 summarizes, for each benchmark, the rendered field used by VLM-based methods and the corresponding average compression ratio. To ensure comparability, we keep the settings in Table 2 fixed within each benchmark and evaluate all methods under the same compression ratio specified in the table. Therefore, performance differences across methods cannot be attributed to different compression ratios, but rather reflect the effectiveness of the methods themselves.

Table 3. CompScore on Long Module Summarization at average compression ratio  $\approx 1.7\times$ . Best results are bolded.

| Model       | Method                    | CompScore    | Ratio       |
|-------------|---------------------------|--------------|-------------|
| Qwen3-8B    | No Compression            | 47.55        | 1.0×        |
|             | Random Line               | 52.07        | 1.7×        |
|             | RAG (Sliding Window)      | 43.05        | 1.7×        |
|             | RAG (Function Chunking)   | 46.34        | 1.7×        |
|             | LongLLMLingua             | 45.76        | 1.7×        |
|             | LLMLingua                 | 48.23        | 1.8×        |
|             | LLMLingua-2               | 58.18        | 1.7×        |
|             | LongCodeZip               | 50.40        | 1.7×        |
| Qwen3-VL-8B | <b>LongCodeOCR (ours)</b> | <b>87.25</b> | <b>1.7×</b> |

Regarding inference, explicit reasoning mode, denoted as “thinking”, is enabled for all evaluated models. The reasoning budget is capped at 2048 tokens; once the cap is reached, the reasoning phase is terminated and the final answer is produced. For all tasks, evaluation is conducted solely on the final outputs, while intermediate reasoning content is excluded. Except for enabling “thinking” and setting the associated budget, decoding parameters and output constraints are kept identical across models to reduce confounding effects introduced by generation strategies.

## 5 Study Results

In this section, we present experimental results and our analysis to answer the research questions.

### 5.1 RQ1: Can visual code compression serve as a viable alternative to textual code compression for long-context understanding?

To assess whether visual code compression can serve as a reliable alternative to textual representations without sacrificing downstream utility, we evaluate our instantiation, LongCodeOCR, on the Long Module Summarization benchmark introduced by LongCodeZip [36]. We adopt this benchmark for three reasons. First, summarization over long repositories is highly sensitive to missing prerequisites and non-local dependencies, making it a stringent testbed for context compression. Second, it provides a standardized evaluation protocol and a broad suite of representative baselines. Third, LongCodeZip reports its most competitive results on this benchmark among the tasks in their study; using the same setting therefore yields a direct and baseline-favorable comparison.

Table 3 reports CompScore together with the achieved average compression ratio for each method. We focus on the target compression strength with a ratio of approximately  $1.7\times$ . Non-visual baselines operate on code tokens and are evaluated with Qwen3-8B. LongCodeOCR renders code as images and is evaluated with a VLM, Qwen3-VL-8B. Overall, LongCodeOCR achieves a substantially higher CompScore than all non-visual baselines at comparable compression ratios, supporting the effectiveness of global-preserving visual code compression under strong compression.

Within non-visual baselines, moderate compression is not necessarily detrimental. Random line sampling at ratio  $1.7\times$  improves CompScore from 47.55 under no compression to 52.07, indicating redundancy in long-context inputs. Retrieval-based variants are less effective in this setting. Sliding-window retrieval achieves 43.05, and function-level chunking reaches 46.34, both below the no-compression baseline. Prompt compression methods exhibit mixed results. LongLLMLingua and

Table 4. Visual code compression versus textual code compression on Long Module Summarization, stratified by input length. Each entry reports CompScore. Compression ratios are approximately comparable ( $\approx 1.7\times$ ). Best results are bolded.  $n$  denotes the number of instances in each length bin.

| Method      | Model       | Input length |               |              | Avg          | Ratio        |
|-------------|-------------|--------------|---------------|--------------|--------------|--------------|
|             |             | 0k-8k (n=64) | 8k-16k (n=31) | 16k+ (n=44)  |              |              |
| LongCodeZip | Qwen3-8B    | 56.47        | 52.56         | 40.06        | 50.40        | 1.7 $\times$ |
| LongCodeOCR | Qwen3-VL-8B | <b>89.09</b> | <b>92.65</b>  | <b>80.76</b> | <b>87.25</b> | 1.7 $\times$ |
|             | Glyph       | 73.49        | 74.29         | 70.56        | 72.74        | 1.7 $\times$ |

LLMLingua obtain 45.76 and 48.23, respectively. LLMLingua-2 yields the strongest performance among non-visual baselines and reaches 58.18. Also, LongCodeZip achieves 50.40 at the target ratio.

LongCodeOCR shows a large advantage at the same compression strength. At ratio 1.7 $\times$ , LongCodeOCR reaches a CompScore of 87.25 and exceeds LLMLingua-2 by 29.07 points. This margin is far larger than the gain from simple redundancy removal, where random line sampling improves by 4.52 points over no compression. These results suggest that representing code in a 2D visual layout can retain task-relevant signals more effectively than keep-or-discard selection on 1D token sequences. In particular, rendering preserves layout cues such as indentation, alignment, and block structure. It also provides a more contiguous view of code regions that may otherwise be fragmented by selective filtering or retrieval.

**Finding 1:** Visual code compression significantly outperforms textual code compression on code summarization at comparable ratios ( $\approx 1.7\times$ ), demonstrating superior preservation of global semantic integrity

## 5.2 RQ2: How does visual code compression compare with textual code compression across tasks and context lengths?

To examine how code compression strategies generalize across tasks and increasing context lengths, we compare LongCodeOCR with a representative textual code compression, LongCodeZip [36] on a suite of long-context code benchmarks. For each task, we stratify evaluation instances by input length and report task-specific performance within each length stratum. We additionally include Glyph[10], a VLM tailored for long-context visual compression, to assess whether LongCodeOCR is effectiveness or robust across both general-purpose and specialized VLMs.

Table 5. Visual code compression versus textual code compression on RepoBench-P, stratified by input length. Each entry reports ES. Compression ratios are approximately comparable ( $\approx 2.0\times$ ). Best results are bolded.  $n$  denotes the number of instances in each length bin.

| Method      | Model       | Input length  |               |              | Avg          | Ratio        |
|-------------|-------------|---------------|---------------|--------------|--------------|--------------|
|             |             | 0k-4k (n=278) | 4k-8k (n=180) | 8k+ (n=42)   |              |              |
| LongCodeZip | Qwen3-8B    | 42.25         | 37.37         | 30.17        | 39.48        | 2.0 $\times$ |
| LongCodeOCR | Qwen3-VL-8B | 52.33         | 47.98         | 45.76        | 50.22        | 2.0 $\times$ |
|             | Glyph       | <b>62.20</b>  | <b>59.88</b>  | <b>53.98</b> | <b>60.68</b> | 2.0 $\times$ |

Table 6. Visual code compression versus textual code compression on LCC, stratified by input length. Each entry reports ES/EM (left/right). Compression ratios are approximately comparable ( $\approx 2.0\times$ ). Best results are bolded.  $n$  denotes the number of instances in each length bin.

| Method      | Model       | Input length         |                      |                      | Avg                  | Ratio        |
|-------------|-------------|----------------------|----------------------|----------------------|----------------------|--------------|
|             |             | 0k-8k (n=275)        | 8k-16k (n=177)       | 16k+ (n=48)          |                      |              |
| LongCodeZip | Qwen3-8B    | 38.48 / 9.45         | 35.14 / 12.99        | 34.68 / 8.33         | 36.93 / 10.60        | 2.0 $\times$ |
| LongCodeOCR | Qwen3-VL-8B | 42.18 / 13.45        | 43.28 / 12.43        | 38.38 / 2.08         | 42.21 / 12.00        | 2.0 $\times$ |
|             | Glyph       | <b>45.56 / 13.45</b> | <b>46.91 / 13.56</b> | <b>44.09 / 14.58</b> | <b>45.90 / 13.60</b> | 2.0 $\times$ |

5.2.1 *Performance Analysis across Diverse Code Task Types.* We compare two compression approaches, visual code compression via LongCodeOCR and textual code compression exemplified by LongCodeZip, using the average (AVG) results across benchmarks in Tables 4–8.

**Code summarization: Global abstraction with long-range dependencies.** Table 4 reveals a substantial advantage for visual compression. Under aligned budgets ( $\approx 1.7\times$ ), LongCodeOCR with Qwen3-VL-8B dominates LongCodeZip (50.40) with a CompScore of **87.25 (+36.85)**. This intrinsic benefit is corroborated by the specialized Glyph (72.74). We attribute these gains to the preservation of global spatial layout, whereas textual code compression risks fragmenting context by discarding globally informative cues. The gap between VLMs further indicates that summarization relies on code-aware semantic organization.

**Code completion: Constraint recovery and symbolic precision.** Under an approximately comparable compression ratio of 2.0 $\times$ , visual code compression consistently improves code completion over textual code compression. On RepoBench-P (Table 5), the average ES increases from 39.48 with LongCodeZip to 50.22 when LongCodeOCR uses Qwen3-VL-8B as the backbone, and further to 60.68 when it uses Glyph; on LCC (Table 6), the average ES/EM increases from 36.93/10.60 to 42.21/12.00 and 45.90/13.60. Mechanistically, discard-based textual code compression incurs irreversible coverage loss that is more damaging when constraints are dispersed across files, whereas visual code compression preserves broader coverage but is bounded by fidelity for fine-grained symbols; a code-specialized visual backbone (Glyph) further mitigates this fidelity bottleneck under exactness requirements.

**Code QA: Evidence-seeking and reasoning over long contexts.** Tables 7 and 8 reveal a regime-dependent competitive landscape where neither paradigm uniformly dominates. In the standard long-context regime (Table 7), LongCodeOCR (Qwen3-VL-8B) maintains a slight edge over LongCodeZip (70.46% vs. 67.61%), while the specialized model Glyph trails at 64.42%. However, the ultra-long regime (Table 8) exposes the superior scalability of visual compression.

While LongCodeZip leads at 512k, a decisive crossover occurs at 1M. Strikingly, Glyph achieves **70.00%** accuracy under an extreme compression ratio of **12.2 $\times$** , significantly outperforming LongCodeZip (64.00%) which operates at a much lower compression of 3.0 $\times$ . Along with Qwen3-VL-8B (72.00%), these results suggest that as context scales to millions of tokens, preserving global visual layout offers higher information density than text filtering, enabling effective evidence retrieval even under severe compression constraints.

**Finding 2:** Visual code compression excels in tasks requiring semantic coverage and constraint grounding, whereas textual code compression is effective for tasks driven by sparse, locally salient evidence.

Table 7. Visual code compression versus textual code compression on LongCodeQA, stratified by input length. Each entry reports accuracy (Acc%). Compression ratios are approximately comparable ( $\approx 1.6\times$ ). Best results are bolded.  $n$  denotes the number of instances in each length bin.

| Method      | Model       | Input length |              |              | Avg          | Ratio        |
|-------------|-------------|--------------|--------------|--------------|--------------|--------------|
|             |             | 32k (n=113)  | 64k (n=76)   | 128k (n=92)  |              |              |
| LongCodeZip | Qwen3-8B    | <b>64.60</b> | 71.05        | 68.48        | 67.61        | 1.6 $\times$ |
| LongCodeOCR | Qwen3-VL-8B | 63.72        | <b>80.26</b> | <b>70.65</b> | <b>70.46</b> | 1.6 $\times$ |
|             | Glyph       | 63.72        | 72.37        | 58.70        | 64.42        | 1.6 $\times$ |

Table 8. Scalability at ultra-long inputs (512k–1M) on LongCodeQA. Each entry reports accuracy (Acc%). Compression ratios vary due to model context limits. Best results are bolded.  $n$  denotes the number of instances in each length bin.

| Method      | Model       | 512k (n=47)  |              | 1M (n=50)    |               |
|-------------|-------------|--------------|--------------|--------------|---------------|
|             |             | Acc%         | Ratio        | Acc%         | Ratio         |
| LongCodeZip | Qwen3-8B    | <b>74.47</b> | 2.8 $\times$ | 64.00        | 3.0 $\times$  |
| LongCodeOCR | Qwen3-VL-8B | 65.96        | 2.8 $\times$ | <b>72.00</b> | 8.1 $\times$  |
|             | Glyph       | 59.57        | 3.7 $\times$ | 70.00        | 12.2 $\times$ |

5.2.2 *Performance Analysis across Varying Code Context Length.* Stratified evaluations across benchmarks indicate that visual code compression is generally more robust to context scaling than selective filtering, while also exposing task-dependent bottlenecks at extreme lengths.

**Robustness against context expansion.** For semantic-heavy tasks, including summarization and repo-level code completion, a consistent pattern emerges as inputs extend to the longest bins: LongCodeZip degrades markedly, whereas LongCodeOCR retains stronger utility. In summarization (Table 4), the textual baseline drops from 56.47 (0k–8k) to 40.06 (16k+), while LongCodeOCR with Qwen3-VL-8B remains at 80.76. A similar trend appears in repo-level code completion (Table 5), where LongCodeZip decreases from 42.25 to 30.17, in contrast to the visual model’s more stable performance (45.76). These divergences are consistent with different degradation mechanisms: textual code compression can induce **context fragmentation** by pruning dispersed yet decisive cues, whereas visual code compression mitigates coverage loss by retaining more global structural information.

**Precision bottlenecks at extreme lengths.** The exactness-sensitive LCC task (Table 6) further highlights a fidelity boundary of visual encoding under high-density inputs. While Glyph remains comparatively stable, Qwen3-VL-8B exhibits a sharp drop in Exact Match in the 16k+ regime (EM: 2.08) despite maintaining moderate semantic similarity (ES: 38.38). This pattern is consistent with a **visual crowding** effect: as context density increases, glyphs become smaller and layouts more crowded, amplifying symbol-level noise. Such noise may have limited impact on coarse semantic similarity, but it becomes a primary bottleneck when strict symbol-level fidelity is required.

**Scalability and budget-sensitive reversal.** Finally, the LongCodeQA benchmark (Tables 7–8) illustrates a regime-dependent shift under feasible budgets. In the standard long-context regime (Table 7), LongCodeOCR attains strong performance at moderate lengths (e.g., 80.26 vs. 71.05 at 64k). More notably, the ultra-long regime (Table 8) reveals a crossover: LongCodeZip leads at 512k

(74.47), whereas LongCodeOCR becomes more competitive at 1M (72.00 vs. 64.00). We interpret this reversal as utility achieved under **fit-in-context budgets**: at million-token scales, where feasibility is constrained by context limits, visual compression can offer higher effective information density than textual code compression.

Table 9. Reference comparison with selected long-context LLMs on LongCodeQA (Acc%) across input lengths. Our result uses LongCodeOCR to compress the input before inference with Qwen3-VL-8B (ratio-matched setting as in RQ2; no task-specific tuning). Best results are bolded.  $n$  denotes the number of instances in each length bin.

| Model                     | 32K (n=113) | 64k (n=76)   | 128k (n=92) | 512k (n=47) | 1M (n=50)    |
|---------------------------|-------------|--------------|-------------|-------------|--------------|
| Llama 3.1 – 405B Instruct | 69.9        | 72.4         | 67.4        | –           | –            |
| GPT-4o                    | 65.5        | 76.3         | <b>74.3</b> | –           | –            |
| Gemini 2.5 Pro            | <b>75.2</b> | 71.1         | 71.7        | <b>68.1</b> | 69.8         |
| Claude 3.5 Sonnet         | 65.5        | 69.7         | 71.7        | –           | –            |
| Claude 3.5 Sonnet + RAG   | 25.55       | 31.18        | 24.83       | 17.19       | 12.77        |
| LongCodeOCR + Qwen3-VL-8B | 63.72       | <b>80.26</b> | 70.65       | 65.96       | <b>72.00</b> |

**Reference comparison with strong open- and closed-source models.** Table 9 provides a reference comparison with representative open- and closed-source models evaluated across input lengths, where these baselines rely on their native context windows. Without task-specific fine-tuning and with compression enabled only at inference time, LongCodeOCR with a lightweight Qwen3-VL-8B backbone achieves competitive accuracy in certain length regimes. Specifically, at 64k input length, it reaches **80.26**, exceeding GPT-4o (76.3) and Llama 3.1-405B Instruct (72.4); at 1M input length, it attains **72.00**, slightly higher than Gemini 2.5 Pro (69.8). These results suggest that, under feasible budget and context constraints, long-code understanding is influenced not only by native context length but also by how the context is represented; visual code compression can serve as a compact representation that improves the utility of ultra-long inputs for evidence seeking and reasoning.

**Finding 3:** Visual code compression scales more stably than textual code compression as context length grows, and its advantage becomes more pronounced for ultra-long inputs.

### 5.3 RQ3: What is the sensitivity of visual code compression to variations in compression ratio and rendering configuration?

We conduct a sensitivity analysis of visual code compression on RepoBench-P[3] and LCC[19] by varying compression ratio and rendering configuration. We evaluate LongCodeOCR with Qwen3-VL-8B and compare against a textual code compression method implemented by LongCodeZip with Qwen3-8B. Due to the high overhead of fine filtering (Table 1), we use coarse filtering only for LongCodeZip.

*Compression-ratio sensitivity.* In terms of performance, LongCodeOCR exhibits remarkable stability on the repository-level task (RepoBench-P), with its Edit Similarity (ES) fluctuating within a narrow range of 3.66 points (47.98–51.64). In contrast, LongCodeZip shows high volatility with a range of 12.85 points, allowing the visual paradigm to maintain a significant lead across compression ratios from 1 $\times$  to 5 $\times$ . However, on the single-file task (LCC), LongCodeOCR displays a monotonic

Table 10. Sensitivity of ES to compression ratio on RepoBench and LCC (4k–8k, 180 instances per benchmark). LongCodeZip uses coarse filtering only. Row-wise maxima are bolded.

| Task        | Method               | 1.0×         | 2.0×         | 3.0×  | 4.0×         | 5.0×  |
|-------------|----------------------|--------------|--------------|-------|--------------|-------|
| RepoBench-P | LongCodeZip (coarse) | 32.75        | 40.86        | 40.44 | <b>45.60</b> | 45.36 |
|             | LongCodeOCR          | 49.56        | 47.98        | 48.48 | <b>51.64</b> | 50.70 |
| LCC         | LongCodeZip (coarse) | 34.03        | <b>35.74</b> | 35.24 | 34.14        | 33.88 |
|             | LongCodeOCR          | <b>42.83</b> | 39.35        | 38.95 | 35.52        | 35.34 |

Table 11. Exploratory analysis of rendering settings. We vary font and layout (single column vs. two column) while keeping all other settings fixed. We report ES on RepoBench-P and both ES/EM on LCC.

| Setting               | RepoBench-P |       | LCC   |    |
|-----------------------|-------------|-------|-------|----|
|                       | ES          | ES    | ES    | EM |
| <i>(a) Font</i>       |             |       |       |    |
| Verdana               | 51.63       | 39.35 | 11.11 |    |
| JetBrainsMono-Regular | 50.98       | 41.75 | 12.78 |    |
| <i>(b) Layout</i>     |             |       |       |    |
| Single column         | 51.63       | 39.35 | 11.11 |    |
| Two column            | 49.19       | 39.77 | 10.00 |    |

degradation as compression intensifies, with a total decrease of 7.49 points, whereas the filtering-based baseline remains relatively flat with a range of only 1.86. Consequently, the performance gap narrows sharply from 8.80 at 1× to 1.46 at 5×, indicating that increasing compression ratios exposes distinct performance bottlenecks for each paradigm.

Mechanistically, this divergence stems from the fundamental difference in the “cost” each paradigm pays for compression. Textual code compression primarily increases the ratio by discarding code units, resulting in irreversible coverage loss. This coverage fragility is particularly detrimental to repository-level tasks where constraints are dispersed and missing a single prerequisite can be fatal; visual code compression mitigates this risk by preserving the global context. Conversely, visual code compression achieves its target by packing nearly the full context into a constrained visual budget, shifting the bottleneck toward visual fidelity. Smaller glyphs and rendering noise impair the resolution of local details required for LCC tasks, thereby diminishing the advantage of visual compression at extreme ratios. This **coverage–fidelity trade-off** explains the sustained superiority of the visual paradigm in broad reasoning scenarios and its potential limitations in local symbolic precision.

*Rendering sensitivity.* LongCodeOCR exhibits task-specific sensitivity to rendering configurations. In RepoBench-P, font choice has a negligible impact (51.63 vs. 50.98), but two-column layouts reduce ES from 51.63 to 49.19. Conversely, LCC is more precision-dependent: JetBrainsMono improves ES/EM by 2.40/1.67 points, while two-column layouts cause EM to drop from 11.11 to 10.00.

This divergence stems from varying visual signal priorities. RepoBench-P is constrained by global structure; it relies on spatial cues like indentation rather than character-level resolution, making it font-insensitive but vulnerable to layout-induced noise. In contrast, LCC performance is limited by visual fidelity for local continuation. Monospaced fonts enhance surface-form reconstruction,

whereas dense layouts introduce character misrecognition, disproportionately harming the strict Exact Match (EM) metric.

**Finding 4:** Visual code compression is governed by a fundamental coverage-fidelity trade-off: it excels in global-dependency tasks by preserving context coverage, but faces a fidelity bottleneck in exactness-critical tasks. While textual code compression pays with structural coverage loss, visual code compression pays with symbolic fidelity loss.

## 6 Discussion and Threats to Validity

### 6.1 Discussion

Our experimental results demonstrate the distinct advantages of visual code compression across various long-context scenarios. To further understand the underlying mechanisms and practical implications of these findings, this section synthesizes our observations into a theoretical framework, analyzes the trade-offs between different paradigms, and discusses the feasibility of deploying such models in real-world software engineering workflows.

**6.1.1 The Coverage–Fidelity Trade-off: Implications for Choosing Compression Paradigms.** Our empirical study identifies a fundamental mechanism governing long-context code understanding: the *coverage–fidelity trade-off*. Textual code compression operate by discretely pruning context, often leading to *coverage loss* where omitting prerequisite constraints irreversibly fragments code logic. In contrast, visual code compression preserves global context via continuous mapping but faces a *fidelity bottleneck* bounded by resolution. This distinction dictates paradigm suitability based on signal distribution: visual code compression dominates in macro-level reasoning (e.g., summarization) where task-critical signals are sparsely dispersed, whereas textual code compression retains a competitive edge in micro-level tasks requiring high symbolic precision. Essentially, the choice entails balancing the risk of structural incompleteness against symbolic ambiguity.

**6.1.2 Cost-Efficiency and Interactive Feasibility.** Beyond accuracy, the shift to visual processing introduces a transformative advantage in deployment feasibility. Achieving high fidelity in selective filtering (e.g., LongCodeZip) typically necessitates expensive model-based metrics, incurring substantial token and latency overheads. Conversely, LongCodeOCR shifts the computational burden from heavy LLM inference to lightweight graphical rendering. This paradigm eliminates compression-stage token consumption and drastically reduces preprocessing latency. Such efficiency unlocks the feasibility of million-token context analysis in resource-constrained, real-time environments such as IDE plugins that remain computationally prohibitive for heavy, model-driven filtering pipelines.

**6.1.3 Future Directions.** Our findings suggest several promising directions for improving the reliability and practicality of visual code compression for long-context code understanding. First, future work can mitigate symbol-level fidelity bottlenecks by exploring resolution-adaptive rendering and symbol-aware layouts, and by incorporating lightweight verification or correction mechanisms to reduce the impact of OCR noise on exactness-critical tasks. Second, hybrid pipelines that combine global-preserving visual views with selective filtering-based compression may better balance the coverage–fidelity trade-off under tight context and latency budgets.

### 6.2 Threats to Validity

While our empirical study provides systematic evidence for the efficacy of visual code compression, several factors may impact the validity of our findings. Following the standard guidelines for

empirical software engineering, we identify and discuss potential threats to validity in terms of internal, external, and construct validity, along with the mitigation strategies we employed.

**6.2.1 Internal Validity.** A potential threat to internal validity concerns the fairness of comparisons across modalities. To ensure a rigorous baseline, we match the compression ratios between visual code compression and textual code compression across all benchmarks. Moreover, to reduce confounding effects related to model family and pretraining, we compare Qwen3-VL-8B with its matched text-only counterpart, Qwen3-8B. Because these models are developed within the same model family and likely share broadly similar pretraining data sources, this controlled comparison helps isolate the effect of visual structural representations from differences in model lineage and data exposure.

**6.2.2 External Validity.** External validity concerns the generalizability of our findings to other tasks and models. We mitigate this threat by evaluating our approach on four representative long-context code benchmarks spanning code summarization, code question answering, and code completion. Moreover, we consider two distinct VLM backbones, Qwen3-VL-8B and Glyph (a specialized 9B VLM), to reduce concerns that the observed benefits of visual compression are specific to a single model. Finally, our RQ3 results indicate robustness across practical rendering configurations, including font types and spatial layouts.

**6.2.3 Construct Validity.** Construct validity concerns whether the benchmark metrics faithfully reflect the intended notion of task correctness, rather than over-emphasizing textual surface forms. For instance, the EM metric in the LCC task is highly sensitive to symbol-level precision and may disproportionately penalize visual pipelines when OCR introduces minor character-level noise. To mitigate potential metric-driven bias, we strictly follow each benchmark’s standardized evaluation protocol and report the metric(s) it specifies. In particular, for LCC we report both strict EM and a softer similarity measure such as ES, as prescribed by the benchmark. This reporting helps avoid over-reliance on a single strict criterion and supports our discussion of the *coverage–fidelity trade-off* between broader context coverage and symbol-level fidelity.

## 7 Related Work

### 7.1 Long-Context Code Benchmarks and Tasks

Code evaluation benchmarks have evolved from standalone function synthesis (typified by HumanEval [6]) to repository-level tasks that require reasoning over cross-file constraints. This shift has motivated long-context benchmarks that assess evidence localization and reasoning consistency under extensive inputs.

In **cross-file completion**, RepoBench [29], CrossCodeEval [15], and RepoEval [46] move beyond local code generation to evaluate project-level context utilization, emphasizing the need to identify dispersed dependencies while controlling data leakage and memorization.

In **long-code understanding and maintenance**, RepoQA [27] and LongCodeU [24] focus on evidence localization and inter-unit relation understanding. LongCodeBench [35] further scales contexts to the million-token level to study degradation under extreme length. In parallel, SWE-bench [22] and Long Code Arena [5] ground evaluation in realistic workflows such as issue resolution and codebase maintenance.

### 7.2 Efficient Long-Context Architectures

The primary bottleneck in processing massive code repositories lies in the quadratic complexity of self-attention [37]. To reduce the prohibitive compute and memory costs of extending context

windows, prior work largely follows two directions: improving architectural efficiency and enabling length extrapolation.

**Architectural Efficiency.** Early studies explored sparse attention patterns [4, 45] and kernel-based linearization [12, 39]. System-level innovations such as FlashAttention [14] further enable efficient exact attention via IO-aware tiling. Compressive and recurrent architectures, including Transformer-XL [13] and Infini-attention [30], maintain bounded memory states to capture long-range dependencies without scaling computation linearly with history length.

**Extrapolation and Utilization.** Robust positional extrapolation is critical for effectiveness beyond training length. ALiBi [34] and RoPE scaling strategies, including YaRN [33] and LongRoPE [16], extend effective context windows post-training. However, longer nominal windows alone do not guarantee reliable utilization; recent work emphasizes data curation and efficient fine-tuning paradigms, including LongLoRA [9] and LongAlign [2], to improve models’ ability to consistently use critical information in long contexts [49].

### 7.3 Context Compression Paradigms

Context compression mitigates the computational burden of long-context modeling by increasing information density under a constrained context budget. Prior work largely follows two paradigms: selective filtering-based compression and cross-modal visual compression.

**Selective filtering-based compression.** General-purpose compressors such as LLMLingua [20, 32] and Selective Context [26] leverage signals including perplexity to identify and remove low-utility content. For source code, however, token removal must respect program structure; otherwise it may violate syntactic well-formedness and disrupt cross-file dependency chains. Code-oriented methods therefore incorporate structure-aware constraints. DietCode [48] and SlimCode [40] utilize syntactic structure and program dependencies to guide selective filtering while maintaining structural fidelity. At repository scale, LongCodeZip [36] provides a systematic pipeline for compressing distributed code contexts and constitutes a strong representative of text-based code compression.

**Cross-modal visual compression.** Vision–text compression (VTC) exploits the visual modality by rendering text into images and encoding them into a fixed number of visual tokens through vision encoders. VIST [43] and VisInContext [38] show that visual representations of low-salience context can reduce token costs while maintaining downstream performance. Related “optical computing” lines of work, including DeepSeek-OCR [41], Glyph [10], and AgentOCR [17], further demonstrate the feasibility of extreme compression for OCR and long-horizon agent histories by leveraging two-dimensional layouts and vision–language models.

## 8 Conclusion

In this paper, we conducted a systematic empirical study to evaluate the efficacy and applicability boundaries of visual code compression relative to textual code compression for long-context code understanding. Under a controlled and identical experimental protocol, we benchmarked LongCodeOCR against representative baselines, including LongCodeZip, across a diverse suite of long-context software engineering tasks. Our results characterize a fundamental coverage–fidelity trade-off inherent in these paradigms: visual code compression favors retaining higher context coverage to support long-range constraints and global evidence integration, thereby exhibiting more stable behavior in scenarios requiring broad semantic coverage. Conversely, textual code compression maintains textual symbolic precision and remains competitive in settings that are highly sensitive to local surface forms under high compression strengths. Furthermore, our analysis indicates that the primary risk of textual code compression stems from coverage loss, whereas the bottleneck of visual code compression is manifested as fidelity degradation affecting fine-grained symbol recognition. Finally, we discuss the implications and offer guidelines on when to prioritize

visual compression and how to navigate the trade-offs between compression strength and rendering configurations.

## References

- [1] Shuai Bai, Yuxuan Cai, Ruizhe Chen, Keqin Chen, Xionghui Chen, Zesen Cheng, Lianghao Deng, Wei Ding, Chang Gao, Chunjiang Ge, Wenbin Ge, Zhifang Guo, Qidong Huang, Jie Huang, Fei Huang, Binyuan Hui, Shutong Jiang, Zhaohai Li, Mingsheng Li, Mei Li, Kaixin Li, Zicheng Lin, Junyang Lin, Xuejing Liu, Jiawei Liu, Chenglong Liu, Yang Liu, Dayiheng Liu, Shixuan Liu, Dunjie Lu, Ruilin Luo, Chenxu Lv, Rui Men, Lingchen Meng, Xuancheng Ren, Xingzhang Ren, Sibo Song, Yuchong Sun, Jun Tang, Jianhong Tu, Jianqiang Wan, Peng Wang, Pengfei Wang, Qiuyue Wang, Yuxuan Wang, Tianbao Xie, Yiheng Xu, Haiyang Xu, Jin Xu, Zhibo Yang, Mingkun Yang, Jianxin Yang, An Yang, Bowen Yu, Fei Zhang, Hang Zhang, Xi Zhang, Bo Zheng, Humen Zhong, Jingren Zhou, Fan Zhou, Jing Zhou, Yuanzhi Zhu, and Ke Zhu. 2025. Qwen3-VL Technical Report. arXiv:2511.21631 [cs.CV] <https://arxiv.org/abs/2511.21631>
- [2] Yushi Bai, Xin Lv, Jiajie Zhang, Yuze He, Ji Qi, Lei Hou, Jie Tang, Yuxiao Dong, and Juanzi Li. 2024. Longalign: A recipe for long context alignment of large language models. *arXiv preprint arXiv:2401.18058* (2024).
- [3] Yushi Bai, Xin Lv, Jiajie Zhang, Hongchang Lyu, Jiankai Tang, Zhidian Huang, Zhengxiao Du, Xiao Liu, Aohan Zeng, Lei Hou, et al. 2024. Longbench: A bilingual, multitask benchmark for long context understanding. In *Proceedings of the 62nd annual meeting of the association for computational linguistics (volume 1: Long papers)*. 3119–3137.
- [4] Iz Beltagy, Matthew E Peters, and Arman Cohan. 2020. Longformer: The long-document transformer. *arXiv preprint arXiv:2004.05150* (2020).
- [5] Egor Bogomolov, Aleksandra Eliseeva, Timur Galimzyanov, Evgeniy Glukhov, Anton Shapkin, Maria Tigina, Yaroslav Golubev, Alexander Kovrigin, Arie Van Deursen, Maliheh Izadi, et al. 2024. Long code arena: a set of benchmarks for long-context code models. *arXiv preprint arXiv:2406.11612* (2024).
- [6] Mark Chen. 2021. Evaluating large language models trained on code. *arXiv preprint arXiv:2107.03374* (2021).
- [7] Silin Chen, Shaolin Lin, Xiaodong Gu, Yuling Shi, Heng Lian, Longfei Yun, Dong Chen, Weiguo Sun, Lin Cao, and Qianxiang Wang. 2025. SWE-Exp: Experience-Driven Software Issue Resolution. CoRR abs/2507.23361 (2025). *arXiv preprint arXiv:2507.23361* (2025).
- [8] Yinghao Chen, Zehao Hu, Chen Zhi, Junxiao Han, Shuiguang Deng, and Jianwei Yin. 2024. Chatunitest: A framework for llm-based test generation. In *Companion Proceedings of the 32nd ACM International Conference on the Foundations of Software Engineering*. 572–576.
- [9] Yukang Chen, Shengju Qian, Haotian Tang, Xin Lai, Zhijian Liu, Song Han, and Jiaya Jia. 2023. Longlora: Efficient fine-tuning of long-context large language models. *arXiv preprint arXiv:2309.12307* (2023).
- [10] Jiale Cheng, Yusen Liu, Xinyu Zhang, Yulin Fei, Wenyi Hong, Ruiliang Lyu, Weihan Wang, Zhe Su, Xiaotao Gu, Xiao Liu, et al. 2025. Glyph: Scaling context windows via visual-text compression. *arXiv preprint arXiv:2510.17800* (2025).
- [11] Xin Cheng, Xun Wang, Xingxing Zhang, Tao Ge, Si-Qing Chen, Furu Wei, Huishuai Zhang, and Dongyan Zhao. 2024. xrag: Extreme context compression for retrieval-augmented generation with one token. *Advances in Neural Information Processing Systems* 37 (2024), 109487–109516.
- [12] Krzysztof Choromanski, Valerii Likhoshesterstov, David Dohan, Xingyou Song, Andreea Gane, Tamas Sarlos, Peter Hawkins, Jared Davis, Afroz Mohiuddin, Lukasz Kaiser, et al. 2020. Rethinking attention with performers. *arXiv preprint arXiv:2009.14794* (2020).
- [13] Zihang Dai, Zhilin Yang, Yiming Yang, Jaime G Carbonell, Quoc Le, and Ruslan Salakhutdinov. 2019. Transformer-xl: Attentive language models beyond a fixed-length context. In *Proceedings of the 57th annual meeting of the association for computational linguistics*. 2978–2988.
- [14] Tri Dao, Dan Fu, Stefano Ermon, Atri Rudra, and Christopher Ré. 2022. Flashattention: Fast and memory-efficient exact attention with io-awareness. *Advances in neural information processing systems* 35 (2022), 16344–16359.
- [15] Yangruibo Ding, Zijian Wang, Wasi Ahmad, Hantian Ding, Ming Tan, Nihal Jain, Murali Krishna Ramanathan, Ramesh Nallapati, Parminder Bhatia, Dan Roth, et al. 2023. Crosscodeeval: A diverse and multilingual benchmark for cross-file code completion. *Advances in Neural Information Processing Systems* 36 (2023), 46701–46723.
- [16] Yiran Ding, Li Lyra Zhang, Chengruidong Zhang, Yuanyuan Xu, Ning Shang, Jiahang Xu, Fan Yang, and Mao Yang. 2024. Longrope: Extending llm context window beyond 2 million tokens. *arXiv preprint arXiv:2402.13753* (2024).
- [17] Lang Feng, Fuchao Yang, Feng Chen, Xin Cheng, Haiyang Xu, Zhenglin Wan, Ming Yan, and Bo An. 2026. AgentOCR: Reimagining Agent History via Optical Self-Compression. *arXiv preprint arXiv:2601.04786* (2026).
- [18] Daya Guo, Shuai Lu, Nan Duan, Yanlin Wang, Ming Zhou, and Jian Yin. 2022. Unixcoder: Unified cross-modal pre-training for code representation. *arXiv preprint arXiv:2203.03850* (2022).
- [19] Daya Guo, Canwen Xu, Nan Duan, Jian Yin, and Julian McAuley. 2023. Longcoder: A long-range pre-trained language model for code completion. In *International Conference on Machine Learning*. PMLR, 12098–12107.

- [20] Huiqiang Jiang, Qianhui Wu, Chin-Yew Lin, Yuqing Yang, and Lili Qiu. 2023. Llmlingua: Compressing prompts for accelerated inference of large language models. *arXiv preprint arXiv:2310.05736* (2023).
- [21] Huiqiang Jiang, Qianhui Wu, Xufang Luo, Dongsheng Li, Chin-Yew Lin, Yuqing Yang, and Lili Qiu. 2024. Longllmlingua: Accelerating and enhancing llms in long context scenarios via prompt compression. In *Proceedings of the 62nd Annual Meeting of the Association for Computational Linguistics (Volume 1: Long Papers)*. 1658–1677.
- [22] Carlos E Jimenez, John Yang, Alexander Wettig, Shunyu Yao, Kexin Pei, Ofir Press, and Karthik Narasimhan. 2023. Swe-bench: Can language models resolve real-world github issues? *arXiv preprint arXiv:2310.06770* (2023).
- [23] Han Li, Yuling Shi, Shaoxin Lin, Xiaodong Gu, Heng Lian, Xin Wang, Yantao Jia, Tao Huang, and Qianxiang Wang. 2025. Swe-debate: Competitive multi-agent debate for software issue resolution. *arXiv preprint arXiv:2507.23348* (2025).
- [24] Jia Li, Xuyuan Guo, Lei Li, Kechi Zhang, Ge Li, Jia Li, Zhengwei Tao, Fang Liu, Chongyang Tao, Yuqi Zhu, et al. 2025. Longcodeu: Benchmarking long-context language models on long code understanding. *arXiv preprint arXiv:2503.04359* (2025).
- [25] Jiaqi Li, Mengmeng Wang, Zilong Zheng, and Muhan Zhang. 2024. Loogle: Can long-context language models understand long contexts?. In *Proceedings of the 62nd Annual Meeting of the Association for Computational Linguistics (Volume 1: Long Papers)*. 16304–16333.
- [26] Yucheng Li, Bo Dong, Frank Guerin, and Chenghua Lin. 2023. Compressing context to enhance inference efficiency of large language models. In *Proceedings of the 2023 conference on empirical methods in natural language processing*. 6342–6353.
- [27] Jiawei Liu, Jia Le Tian, Vijay Daita, Yuxiang Wei, Yifeng Ding, Yuhan Katherine Wang, Jun Yang, and Lingming Zhang. 2024. Repoqa: Evaluating long context code understanding. *arXiv preprint arXiv:2406.06025* (2024).
- [28] Nelson F Liu, Kevin Lin, John Hewitt, Ashwin Paranjape, Michele Bevilacqua, Fabio Petroni, and Percy Liang. 2024. Lost in the middle: How language models use long contexts. *Transactions of the Association for Computational Linguistics* 12 (2024), 157–173.
- [29] Tianyang Liu, Canwen Xu, and Julian McAuley. 2023. Repobench: Benchmarking repository-level code auto-completion systems. *arXiv preprint arXiv:2306.03091* (2023).
- [30] Tsendsuren Munkhdalai, Manaal Faruqui, and Siddharth Gopal. 2024. Leave no context behind: Efficient infinite context transformers with infini-attention. *arXiv preprint arXiv:2404.07143* 101 (2024).
- [31] OpenAI. 2024. GPT-4o System Card. *arXiv:2410.21276* [cs.CL] <https://arxiv.org/abs/2410.21276>
- [32] Zhuoshi Pan, Qianhui Wu, Huiqiang Jiang, Menglin Xia, Xufang Luo, Jue Zhang, Qingwei Lin, Victor Rühle, Yuqing Yang, Chin-Yew Lin, et al. 2024. Llmlingua-2: Data distillation for efficient and faithful task-agnostic prompt compression. *arXiv preprint arXiv:2403.12968* (2024).
- [33] Bowen Peng, Jeffrey Quesnelle, Honglu Fan, and Enrico Shippole. [n. d.]. Yarn: Efficient context window extension of large language models, 2023. URL <https://arxiv.org/abs/2309.00071> ([n. d.]).
- [34] Ofir Press, Noah A Smith, and Mike Lewis. 2021. Train short, test long: Attention with linear biases enables input length extrapolation. *arXiv preprint arXiv:2108.12409* (2021).
- [35] Stefano Rando, Luca Romani, Alessio Sampieri, Luca Franco, John Yang, Yuta Kyuragi, Fabio Galasso, and Tatsunori Hashimoto. 2025. LongCodeBench: Evaluating Coding LLMs at 1M Context Windows. *arXiv preprint arXiv:2505.07897* (2025).
- [36] Yuling Shi, Yichun Qian, Hongyu Zhang, Beijun Shen, and Xiaodong Gu. 2025. LongCodeZip: Compress Long Context for Code Language Models. *arXiv preprint arXiv:2510.00446* (2025).
- [37] Ashish Vaswani, Noam Shazeer, Niki Parmar, Jakob Uszkoreit, Llion Jones, Aidan N Gomez, Łukasz Kaiser, and Illia Polosukhin. 2017. Attention is all you need. *Advances in neural information processing systems* 30 (2017).
- [38] Alex Jinpeng Wang, Linjie Li, Yiqi Lin, Min Li, Lijuan Wang, and Mike Zheng Shou. 2024. Leveraging visual tokens for extended text contexts in multi-modal learning. *Advances in Neural Information Processing Systems* 37 (2024), 14325–14348.
- [39] Sinong Wang, Belinda Z Li, Madian Khabsa, Han Fang, and Hao Ma. 2020. Linformer: Self-attention with linear complexity. *arXiv preprint arXiv:2006.04768* (2020).
- [40] Yan Wang, Xiaoning Li, Tien N Nguyen, Shaohua Wang, Chao Ni, and Ling Ding. 2024. Natural is the best: Model-agnostic code simplification for pre-trained large language models. *Proceedings of the ACM on Software Engineering* 1, FSE (2024), 586–608.
- [41] Haoran Wei, Yaofeng Sun, and Yukun Li. 2025. Deepseek-ocr: Contexts optical compression. *arXiv preprint arXiv:2510.18234* (2025).
- [42] Zixuan Wu, Chen Zhi, Junxiao Han, Shuiguang Deng, and Jianwei Yin. 2025. LLMApHub: A Large Collection of LLM-based Applications for the Research Community. In *Proceedings of the 33rd ACM International Conference on the Foundations of Software Engineering*. 1254–1255.
- [43] Ling Xing, Alex Jinpeng Wang, Rui Yan, Xiangbo Shu, and Jinhui Tang. 2025. Vision-centric Token Compression in Large Language Model. *arXiv preprint arXiv:2502.00791* (2025).

- [44] An Yang, Anfeng Li, Baosong Yang, Beichen Zhang, Binyuan Hui, Bo Zheng, Bowen Yu, Chang Gao, Chengan Huang, Chenxu Lv, Chujie Zheng, Dayiheng Liu, Fan Zhou, Fei Huang, Feng Hu, Hao Ge, Haoran Wei, Huan Lin, Jialong Tang, Jian Yang, Jianhong Tu, Jianwei Zhang, Jianxin Yang, Jiaxi Yang, Jing Zhou, Jingren Zhou, Junyang Lin, Kai Dang, Keqin Bao, Kexin Yang, Le Yu, Lianghao Deng, Mei Li, Mingfeng Xue, Mingze Li, Pei Zhang, Peng Wang, Qin Zhu, Rui Men, Ruize Gao, Shixuan Liu, Shuang Luo, Tianhao Li, Tianyi Tang, Wenbiao Yin, Xingzhang Ren, Xinyu Wang, Xinyu Zhang, Xuancheng Ren, Yang Fan, Yang Su, Yichang Zhang, Yinger Zhang, Yu Wan, Yuqiong Liu, Zekun Wang, Zeyu Cui, Zhenru Zhang, Zhipeng Zhou, and Zihan Qiu. 2025. Qwen3 Technical Report. arXiv:2505.09388 [cs.CL] <https://arxiv.org/abs/2505.09388>
- [45] Manzil Zaheer, Guru Guruganesh, Kumar Avinava Dubey, Joshua Ainslie, Chris Alberti, Santiago Ontanon, Philip Pham, Anirudh Ravula, Qifan Wang, Li Yang, et al. 2020. Big bird: Transformers for longer sequences. *Advances in neural information processing systems* 33 (2020), 17283–17297.
- [46] Fengji Zhang, Bei Chen, Yue Zhang, Jacky Keung, Jin Liu, Daoguang Zan, Yi Mao, Jian-Guang Lou, and Weizhu Chen. 2023. Repocoder: Repository-level code completion through iterative retrieval and generation. *arXiv preprint arXiv:2303.12570* (2023).
- [47] Kexun Zhang, Danqing Wang, Jingtao Xia, William Yang Wang, and Lei Li. 2023. Algo: Synthesizing algorithmic programs with generated oracle verifiers. *Advances in Neural Information Processing Systems* 36 (2023), 54769–54784.
- [48] Zhaowei Zhang, Hongyu Zhang, Beijun Shen, and Xiaodong Gu. 2022. Diet code is healthy: Simplifying programs for pre-trained models of code. In *Proceedings of the 30th ACM Joint European Software Engineering Conference and Symposium on the Foundations of Software Engineering*. 1073–1084.
- [49] Hongbo Zhao, Meng Wang, Fei Zhu, Wenzhuo Liu, Bolin Ni, Fanhu Zeng, Gaofeng Meng, and Zhaoxiang Zhang. 2025. VTCBench: Can Vision-Language Models Understand Long Context with Vision-Text Compression? *arXiv preprint arXiv:2512.15649* (2025).